Stoichiometric changes in lithium conducting materials based on $Li_{1+x}Al_xTi_{2-x}(PO_4)_3$: impedance, X-ray and NMR studies

A.S. Best[a,b], M. Forsyth[a,*], D.R. MacFarlane[b]

[a]Department of Materials Engineering, Monash University, Clayton, Victoria 3168, Australia
[b]Department of Chemistry, Monash University, Clayton, Victoria 3168, Australia

Abstract

The lithium fast-ion conductor, $Li_{1+x}Al_xTi_{2-x}(PO_4)_3$ (LATP) has been modified via changes in stoichiometry during the processing steps. The resultant changes have been followed using ^{27}Al MAS NMR, X-ray powder diffraction and impedance spectroscopy. The most important changes were those of the form $Li_{1.3+4y}Al_{0.3}Ti_{1.7-y}(PO_4)_3$. It was possible to remove the $AlPO_4$ phase (both tridymite and berlinite polymorphs), as monitored by X-ray diffractograms and ^{27}Al NMR spectra. Consequently, these changes appear to result in increased grain boundary conductivity of the LATP material. © 2000 Elsevier Science B.V. All rights reserved.

Keywords: LATP; Conductivity; X-ray powder diffraction; Solid state nuclear magnetic resonance

1. Introduction

Lithium Titanium Phosphate $LiTi_2(PO_4)_3$ is a solid electrolyte for possible use in lithium electrochemical applications [1]. The material is based upon the NASICON framework which consists of $[PO_4]$ tetrahedra connected in a corner sharing arrangement with TiO_6 octahedra, which is shown in Fig. 1. This structure provides two sites for conduction; the M_1 site which is understood to be the major pathway and a second smaller site, the M_2 site. Lithium ions are understood to move via interstitial positions between the tetrahedra in the M_1 sites [2,3].

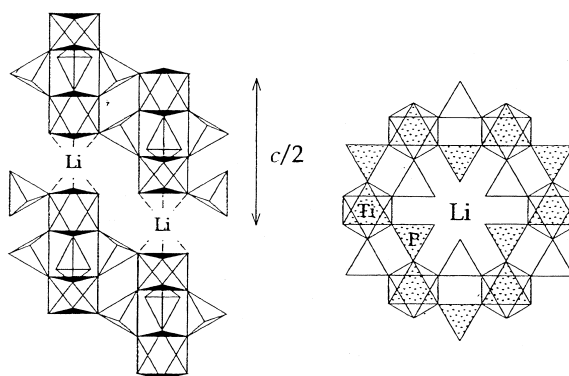By substitution of Al^{3+} ions for Ti^{4+} in the structure to give $Li_{1+x}Al_xTi_{2-x}(PO_4)_3$, Aono et al.

Fig. 1. A representation of the NASICON structure of $LiTi_2(PO_4)_3$ (adopted from Ref. [3]), showing the unit cell stacking along the *c*-axis (left) and its projection onto the basal plane right. Lithium cations occupy the interstitial positions between the six phosphate tetrahedra connected by titanium octahedra.

increased the conductivity over unsubstituted LTP by three orders of magnitude, mainly via improvements in the density and sinterability [4]. Recent studies have shown that LATP has a bulk conductivity of between 2×10^{-3} and 3×10^{-3} S cm^{-1}, but this is accompanied by a grain boundary conductivity of 10^{-5}–10^{-7} S cm^{-1} due to porosity and poor grain boundary sintering.

Many earlier reports have shown that the addition of glassy components (in the batch as starting materials) and varying sintering temperatures, influences the amount of impurity phases present in the material [5,6]. This affects the bulk conductivity due to variation in the 'real stoichiometry' of the material as well as the effect of second phases on the grain boundary conductivity. Four new phases could be identified along with the polycrystalline NASICON-type material, namely $AlPO_4$ (the tridymite and berlinite polymorphs), TiO_2 (rutile) and TiP_2O_7. We hypothesised that $AlPO_4$ may provide a lower energetic pathway for Li$^+$ motion across the grain boundary [7]. However, rutile is a known insulator and the presence of this material may counteract any beneficial effect of other phases on conductivity.

This work aims to clarify the roles of the impurity phases, by controlling the amount of residual rutile, TiP_2O_7 and possibly $AlPO_4$ present within the material through varying the relative ratios of Li, Ti and P in the starting material. X-ray powder diffraction, solid state NMR and impedance studies were used for characterising the final products.

2. Experimental

The synthesis method is as per previous work [5], using a sintering temperature of 1000°C for 3 h, which we have found to be optimal for this system. The faces of the ceramic pellets for impedance analysis were gold sputtered and then silver electrodes were painted onto them. The samples were then subsequently dried at 150°C to ensure any absorbed moisture or solvent was removed. Samples were sealed in gas tight brass cells under nitrogen before measurement. Impedance was measured on a Hewlett Packard 4192A LCR meter between 20 Hz and 1 MHz using 100 mV signal level.

X-ray characterisation was performed on a Rigaku (Giegerflex) spectrometer at room temperature be-

tween $2\theta = 10°$ and 80°. Samples were measured in the powdered state. Solid state NMR measurements were carried on a Bruker MSL 400 spectrometer with an operating frequency of 104.2 MHz. Samples were referenced using a YAG secondary standard at -15 ppm ($[Al(OH_2)_6]^{3+}$ being the primary standard). Room temperature magic angle spinning (MAS) spectra were acquired using a Bruker 4 mm MAS probe (zirconia rotor with Kel-F endcap), at a maximum spinning speed of 10 kHz. 3 νs pulse lengths were typically used, with a recycle delay of 5 s.

3. Results

3.1. X-ray powder diffraction

Fig. 2 shows typical XRD traces of samples from each of the groups referred to in Table 1. Major reflections were assigned according to the previously reported powder diffraction pattern for LTP [8]. The main reaction product has been confirmed to be rhombohedral of space group R_3-c (analogous to NASICON). Previous work has identified that the polycrystalline LATP (group I) material has several secondary phases present, namely, $AlPO_4$ (tridymite and berlinite polymorphs), TiO_2 and TiP_2O_7. A decrease in the unit cell volume from that of LTP was also noted, due to the substitution of a smaller metal ion for Ti^{4+}.

Stoichiometric changes in group II appear to favour the greater formation of the above phases. Within group III, the peaks attributable to $AlPO_4$ (tridymite polymorph) at $2\theta = 21.7°$ and 35.7° are no longer readily observable. The intensity of the TiO_2 peaks also decreases significantly, however TiP_2O_7 peaks are still present. Group IV materials also show the presence of phases seen in groups I and II, in some instances with increased intensity.

The effect of the substitutions undertaken in this work on the unit cell volume can be seen in Table 1. The most significant changes appear to be those within group III, where there is a sharp drop in the unit cell volume as more Ti^{4+} is removed from the structure and more Li$^+$ is added. Changes within groups II and IV appear only to slightly decrease the unit cell volume compared to those changes in groups I and III.
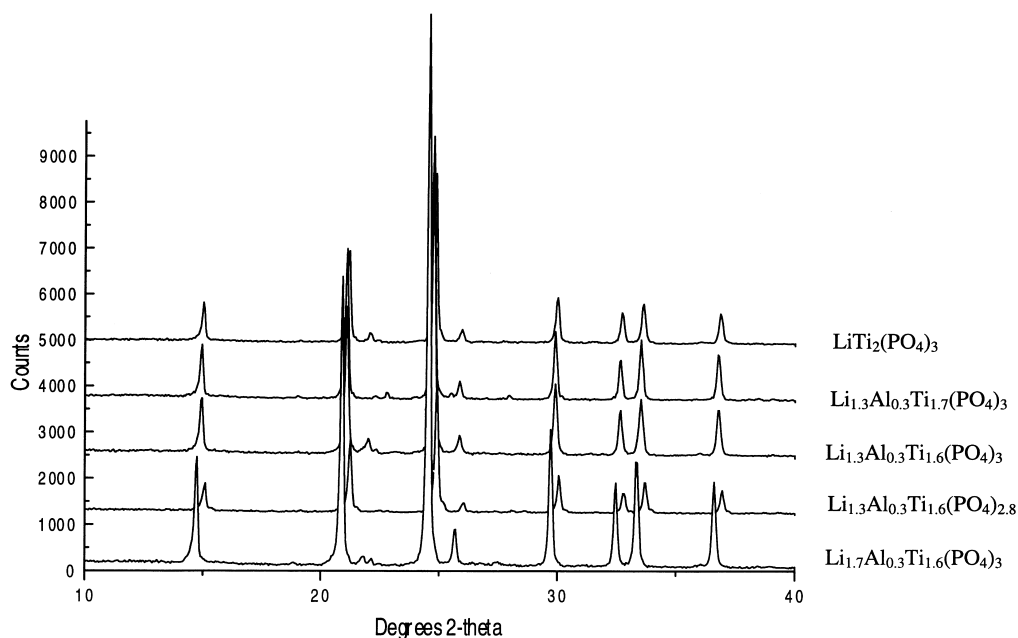
Fig. 2. X-ray diffractograms showing (from top to bottom) LTP, LATP, group II, group IV and group III substitutions (refer to Table 1) in this work.

Table 1
Unit cell parameters for LTP and modified LATP based ceramics

Group	Nominal composition	Substitution	$a/Å$	$c/Å$	$β/°$	$V/Å^3$
I	$LiTi_2(PO_4)_3$ [7]		8.5129	20.878	120	1310.3
	$Li_{1+x}Al_xTi_{2-x}(PO_4)_3$	$x = 0.3$	8.50	20.82	120	1303
II	$Li_{1.3}Al_{0.3}Ti_{1.7-y}(PO_4)_3$	$y = 0.05$	8.50	20.80	120	1300
	$Li_{1.3}Al_{0.3}Ti_{1.7-y}(PO_4)_3$	$y = 0.1$	8.48	20.76	120	1293
III	$Li_{1.3+4y}Al_{0.3}Ti_{1.7-y}(PO_4)_3$	$y = 0.05$	8.48	20.77	120	1292
	$Li_{1.3+4y}Al_{0.3}Ti_{1.7-y}(PO_4)_3$	$y = 0.1$	8.46	20.69	120	1282
	$Li_{1.3+4y}Al_{0.3}Ti_{1.7-y}(PO_4)_3$	$y = 0.15$	8.47	20.72	120	1288
	$Li_{1.3+4y}Al_{0.3}Ti_{1.7-y}(PO_4)_3$	$y = 0.2$	8.48	20.76	120	1292
IV	$Li_{1.3}Al_{0.3}Ti_{1.7-y}(PO_4)_{3-y}$	$y = 0.05$	8.48	20.73	120	1291
	$Li_{1.3}Al_{0.3}Ti_{1.7-y}(PO_4)_{3-y}$	$y = 0.1$	8.50	20.80	120	1301

3.2. ^{27}Al MAS NMR spectroscopy

Fig. 3 shows the spectra obtained for substitutions in group II (refer to Table 1). As can be seen, there are three readily observable peaks: -15 ppm, assigned to octahedral aluminium; 15 ppm, assigned to 5 co-ordinate aluminium; and 40 ppm, assigned to tetrahedral aluminium [6]. From our previous work,

the octahedral peak is attributed to Al within the LATP structure, while the tetrahedral peak is due to the secondary phase $AlPO_4$. The broad peak noted at 15 ppm, ascribed to 5 co-ordinate Al, has not been discussed in our previous work. Due to the broad nature of the peak, we believe this to be an amorphous phase within the polycrystalline NASICON-type material. These substitutions appear to favour
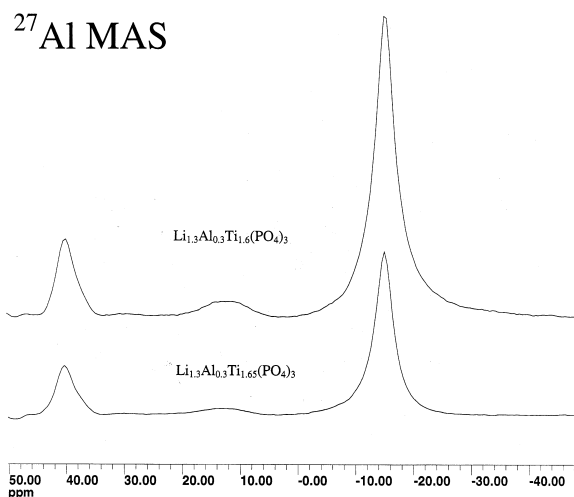
^{27}Al MAS

$Li_{1.3}Al_{0.3}Ti_{1.6}(PO_4)_3$

$Li_{1.3}Al_{0.3}Ti_{1.65}(PO_4)_3$

Fig. 3. ^{27}Al MAS NMR spectra for the substitions in group II, decreasing Ti from bottom to top.

^{27}Al MAS

$Li_{2.1}Al_{0.3}Ti_{1.5}(PO_4)_3$

$Li_{1.9}Al_{0.3}Ti_{1.55}(PO_4)_3$

$Li_{1.7}Al_{0.3}Ti_{1.6}(PO_4)_3$

$Li_{1.5}Al_{0.3}Ti_{1.65}(PO_4)_3$

Fig. 4. ^{27}Al MAS NMR spectra for the substitution in group III, increasing Li and decreasing Ti from bottom to top.

^{27}Al MAS

$Li_{1.3}Al_{0.3}Ti_{1.6}(PO_4)_{2.8}$

$Li_{1.3}Al_{0.3}Ti_{1.6}(PO_4)_{2.9}$

$Li_{1.3}Al_{0.3}Ti_{1.65}(PO_4)_{2.95}$

Fig. 5. ^{27}Al MAS NMR spectra for the substitution in group IV, with decreasing Ti and P from bottom to top.

the formation of the tetrahedral and 5 co-ordinate Al phases due to the strength of intensity of these peaks when compared to that of the octahedral Al peak.

For substitutions in group III, we see a very small peak at 40 ppm (Fig. 4) assigned as tetrahedral Al. This is consistent with X-ray diffractograms showing no peaks attributable to the $AlPO_4$ phase. There is a very small broad peak at 15 ppm, again an amorphous Al phase, but due to the weak intensity of this peak, this phase also could not be identified in X-ray scans. From this spectra, we conclude that nearly all the Al^{3+} within the polycrystalline sample is located within the LATP structure.

Fig. 5 shows the spectra for the substitutions in group IV. In all cases, there are peaks for tetrahedral, 5 co-ordinate and octahedral Al. As more Ti^{4+} and $[PO_4]^{3-}$ species are removed from the LATP material, the intensity of the peaks at 15 and 40 ppm appear to be decreasing with the concomitant increase in the octahedral peak intensity, suggesting more Al is present in the LATP structure.

3.3. Conductivity

Fig. 6 shows the bulk and grain boundary conductivities for a range of modifications to the LATP composition. The largest changes in the grain boundary and bulk conductivities were observed for 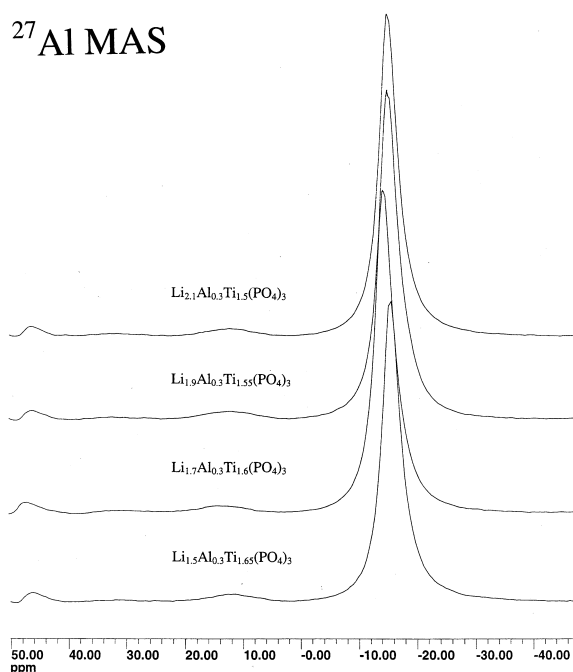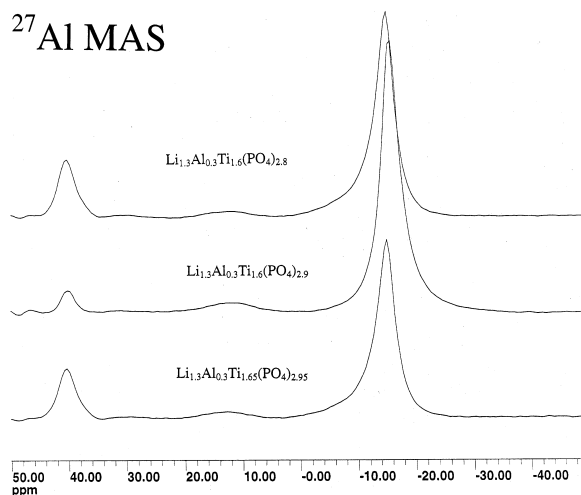the group III system. When $y = 0.1$, the grain boundary conductivity reaches a maximum of 7×10^{-5} S cm^{-1} with a bulk conductivity of 2×10^{-3} S cm^{-1}. Further substitution of Li for Ti did not yield any significant improvements in conductivity.
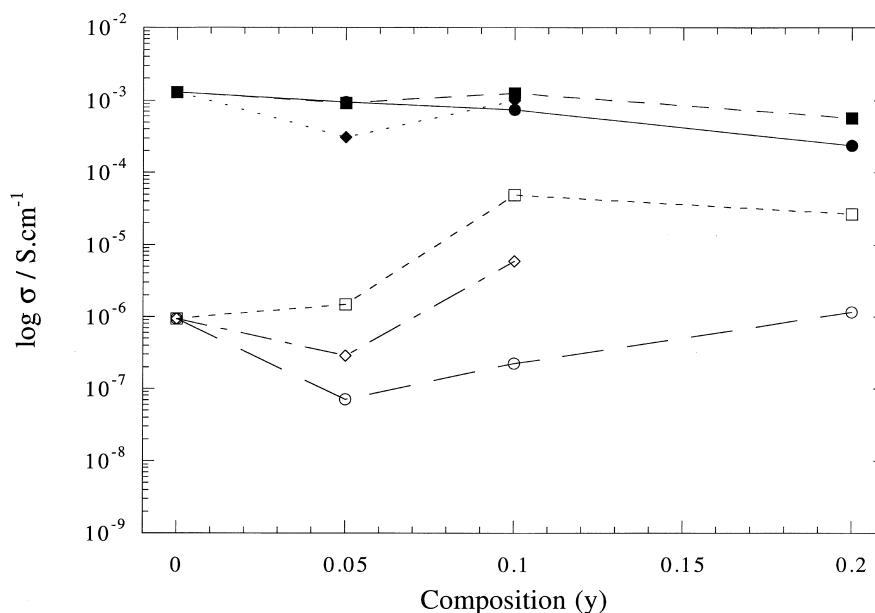
Fig. 6. Grain boundary and bulk conductivity data as a function of composition for substitutions in groups II (open diamonds: grain boundary; closed diamonds: bulk conductivity), group III (open squares: grain boundary; closed squares: bulk conductivity) and group IV (open circles: grain boundary; closed circles: bulk conductivity).

Reduction in the Ti^{4+} content of the material (group II) increases the grain boundary and bulk conductivities at $y = 0.1$. Changing the Ti^{4+} and $[PO_4]^{3-}$ (group IV) content of the material decreases the grain boundary and bulk conductivities for all substitutions in this work.

4. Discussion

The identification of secondary phases has been crucial to the understanding of how the grain boundary conductivity can be modified [6]. We have now been able to reduce the formation of $AlPO_4$ in the polycrystalline sample by substitutions of the form $Li_{1.3+4y}Al_{0.3}Ti_{1.7-y}(PO_4)_3$. When $y = 0.1$ in this system, the grain boundary conductivity reaches a maximum of 5×10^{-5} S cm^{-1}, higher than that of our previous reports. At $y = 1.5$, the grain boundary conductivity is still relatively high compared to that of LATP and those materials with added glass formers [5].

Reducing the Ti content alone and Ti and P together does not appear to optimise conditions for

conduction within the polycrystalline material. This is probably due to the extensive presence of phases such as TiO_2, TiP_2O_7, $AlPO_4$. Due to the broad nature of the 5 co-ordinate peak in the ^{27}Al NMR spectra, this phase is understood to be amorphous in character, possibly an intergranular phase. These five phases appear to reduce the grain boundary conductivity, contrary to the hypothesis that secondary phases may provide lower energetic pathways for lithium ion conduction.

5. Conclusion

We have shown in this work that it is possible to remove the $AlPO_4$ phase from the poly-crystalline ceramic based on $Li_{1.3+4y}Al_{0.3}Ti_{1.7-y}(PO_4)_3$. The removal of this phase is coupled with an increase in the grain boundary conductivity of the material. However, the bulk conductivity of these systems is not higher than that of LATP at any time. Other changes to the basic stoichiometry of $Li_{1.3}Al_{0.3}Ti_{1.7}(PO_4)_3$, did not reduce or remove the presence of the other phases, namely TiO_2, TiP_2O_7

or $AlPO_4$. From ^{27}Al MAS spectra, we have identified an amorphous 5 co-ordinate Al phase which has not been reported in our previous work. We believe that the presence of secondary phases is not needed for the densification or sintering of the final ceramic product. Instead, these phases act as regions of significant resistance which reduce the total conductivity of the final material.

Acknowledgements

References

[1] G.-Y. Adachi, N. Imanaka, H. Aono, Adv. Mater. 8 (1996) 127.

[2] J.B. Goodenough, H.Y.-P. Hong, J.A. Kafalas, Mater. Res. Bull. 11 (1976) 703.

[3] H. Aono, E. Sugimoto, Y. Sadaoka, N. Imanaka, G.-Y. Adachi, J. Elctrochem. Soc. 136 (1989) 590.

[4] H. Aono, E. Sugimoto, Y. Sadaoka, N. Imanaka, G.-Y. Adachi, J. Electrochem. Soc. 140 (1993) 1827.

[5] J. Kuwano, N. Sato, M. Kato, K. Takano, Solid State Ionics 70/71 (1994) 332.

[6] A.S. Best, K.M. Nairn, P.J. Newman, D.R. MacFarlane, M. Forsyth, M.J.G. Jak, J. Austral. Ceram. Soc. 34 (1998) 236–241.

[7] S. Wong, P.J. Newman, A.S. Best, K.M. Nairn, D.R. MacFarlane, M. Forsyth, J. Mater. Chem. 8 (1998) 2199–2203.

[8] Nat Bur Stand U.S. Monogr. 25 (1984) 79.